Available online at www.sciencedirect.com
SCIENCE DIRECT®
International Journal of Heat and Fluid Flow 27 (2006) 54–64
International Journal of HEAT AND FLUID FLOW
www.elsevier.com/locate/ijhff

LES benchmark study of high cycle temperature fluctuations caused by thermal striping in a mixing tee

Lin-Wen Hu *, Mujid S. Kazimi

Massachusetts Institute of Technology, 77 Massachusetts Ave., Cambridge, MA 02139, USA

Received 16 February 2005; received in revised form 20 July 2005
Available online 9 September 2005

Abstract

Thermal striping is identified as one of the causes of thermal fatigue failure in nuclear power plants. Numerical studies of thermal striping require three-dimensional, unsteady turbulent modeling that resolves both large and small-scale turbulent motions. Benchmark studies were carried out using the LES turbulence model solved by the commercial CFD code FLUENT. Two types of mixing tee configurations were modeled to evaluate the performance of the CFD code. The simulation results presented in normalized average temperature and normalized fluctuating temperatures are in good agreement with measurements.

Keywords: Turbulence; Thermal striping; Large eddy simulation

1. Introduction

Prediction of thermal fatigue in mixing tees is a challenging subject that is needed for life management of nuclear power reactor piping systems. Thermal striping is one of the phenomena that have been identified as the cause of thermal fatigue failure. Thermal striping characterizes the phenomenon where hot and cold flow streams join and result in temperature fluctuations of the mixing coolant near a piping wall. The coolant temperature fluctuations may cause cyclical thermal stresses and subsequent fatigue cracking of the pipe wall. Coolant temperature oscillations due to thermal striping are of relatively high frequencies, reported previously to be on the order of several Hz (Wakamatsu et al., 1995).

Studies of thermal striping were initially carried out for liquid-metal-cooled fast breeder reactor (LMFBR) in the 1980's because of the high thermal conductivity of the liquid metal coolant (Muramatsu and Ninikata, 1996). Areas susceptible to thermal striping include components in the core outlet region, such as core upper plenum, flow guide tube, and control rod upper guide tubes. Outside the core region, components where hot and cold streams come in contact, such as tee junctions, elbows, and leakage from valves, may also be affected. The focus of thermal striping studies shifted to light water reactors (LWRs) after several incidents of piping failure at some nuclear power plants (Kim et al., 1993; Claude, 2003; Fukuda et al., 2003). The piping systems that are most susceptible to thermal striping fatigue cracking are mixing tees of the residual heat removal (RHR) systems in both BWR and PWR.

The primary goal of thermal striping evaluation is to identify the coolant fluctuation magnitude and frequencies. This can be achieved by mock-up experiments or three-dimensional, unsteady turbulent modeling that resolves both large and small-scale turbulent motions. This requires computational fluid dynamics (CFD) simulations using either direct numerical simulation (DNS) or large eddy simulations (LES). Thermal

* Corresponding author. Tel.: +1 617 258 5860; fax: +1 617 253 7300.
E-mail address: lwhu@mit.edu (L.-W. Hu).

0142-727X/$ - see front matter © 2005 Elsevier Inc. All rights reserved.
doi:10.1016/j.ijheatfluidflow.2005.08.001

striping experiments were performed previously using flow visualization, temperature measurements, and velocity measurements. In experiments where coolant and pipe wall temperatures were measured, both frequencies and magnitudes of temperature fluctuations can be obtained at selected locations in the pipes. There are few studies related to the analytical approach or computer modeling of thermal striping due to the extensive computational capacity required for unsteady, three-dimensional turbulent flow simulations. Thermal striping was modeled previously using LES and DNS (Muramatsu and Ninikata, 1996; Roubin, 1998; Ohtsuka et al., 2003). However, these studies were performed for only a small volume (subdomain) around the mixing zone due to constraints of large computer memory requirements. Selection of the subdomain and associated boundary conditions plays an important role in such numerical analysis.

2. Large eddy simulation (LES) turbulence model

A general purpose computational fluids dynamics (CFD) code, FLUENT, is chosen for the fluid dynmaics simulation of thermal striping. FLUENT is a state-of-the-art CFD software for modeling fluid flow and heat transfer in complex geometries. It provides a wide range of turbulent models range from k–ε models to the large eddy simulation (LES) model.

LES is a three-dimensional, time-dependent turbulence model which solves the large-scale eddies directly. A filtering operation is applied to the Navier–Stokes equations to decompose the parameter of interest (e.g, velocity) into a filtered component and a residual component. The filtered component represents the large-scale turbulence motions which are strongly influenced by the geometry and boundary conditions. The residual component represents small-scale eddy motion which is determined by the rate of energy transport from large-scale eddies and viscosity. The large eddies are solved explicitly by the filtered Navier–Stokes equations, and the small eddies are modeled using a sub-grid scale (SGS) model. The derivation of filtered Navier–Stokes equations can be found in turbulence textbooks (e.g., Pope, 2000).

Subgrid-scale stresses resulting from the filtering operation are unknown and require modeling. The subgrid-scale (SGS) models that are mostly used are eddy-viscosity models of the following form:

$$\tau_{ij} - \frac{1}{3}\tau_{kk}\delta_{ij} = -2\mu_t \overline{S}_{ij} \tag{1}$$

where μ_t is the SGS turbulent viscosity, and $\overline{S}_{ij}$ is the rate-of-strain tensor for the resolved scale defined by

$$\overline{S}_{ij} = \frac{1}{2}\left(\frac{\partial \overline{u}_i}{\partial x_j} + \frac{\partial \overline{u}_j}{\partial x_i}\right) \tag{2}$$

The first SGS model was proposed by Smagorinsky (1963) and further developed by Lilly (1966). In the Smagorinsky–Lilly model, the turbulent viscosity is modeled by

$$\mu_t = \rho L_s^2 \left|\overline{S}\right| \tag{3}$$

where L_s is the mixing length for subgrid scales and $\left|\overline{S}\right| = \sqrt{2\overline{S}_{ij}\overline{S}_{ji}}$. L_s can be computed using

$$L_s = \min\left(\kappa d, C_s V^{1/3}\right) \tag{4}$$

where $\kappa = 0.42$, d is the distance to the closest wall, C_s is the Smagorinsky constant, and V is the volume of the computational cell.

Lilly (1966) derived a value of 0.23 for C_s from homogeneous isotropic turbulence in the inertial subrange. However, this value was found to cause excessive damping of large-scale fluctuations in the presence of mean shear or in transitional flows. The default value of C_s adopted by the FLUENT code is 0.1, which was found to yield the best results for a wide range of flow conditions.

The other SGS model that was evaluated for the current study is the RNG-based subgrid-scale model. This model is based on the Renormalization Group (RNG) theory that was used to derive the subgrid-scale eddy viscosity model. The RNG procedure results in an effective subgrid viscosity, μ_{eff}, given by

$$\mu_{eff} = \mu + \mu_t \tag{5}$$

and

$$\mu_{eff} = \mu\left[1 + H\left(\frac{\mu_s^2 \mu_{eff}}{\mu^3} - C\right)\right]^{1/3} \tag{6}$$

where $\mu_s = \rho\left(C_{rng} V^{1/3}\right)^2 \left|\overline{S}\right|$, and $H(x)$ is the Heaviside function defined as:

$$H(x) = x \text{ when } x > 0, \quad \text{and} \quad H(x) = 0 \text{ when } x \leqslant 0$$

Yakhot et al. (1989) derived $C_{rng} = 0.157$ and $C = 100$ which are used in the current study. In low-Reynolds-number regions of the flow, the effective viscosity becomes the molecular viscosity. This allows modeling the low-Reynolds-number effects encountered in transitional flows and near-wall regions. In a highly turbulent region where $\mu_{eff} \gg \mu$, the RNG-based subgrid-scale model reduces to the Smagorinsky–Lilly model. Comparisons of initial simulation results using the Smagorinsky and the RNG–SGS models found that the latter was in better agreement with the experimental data (Hu et al., 2003). Therefore, the RNG–SGS model was used in the analyses presented in this paper.

3. Thermal striping experiments

The thermal striping experiments that are used for our benchmark studies were performed by a Japanese

working group which aimed to help the Japan Society for Mechanical Engineers (JSME) establish guidelines for high-cycle fatigue (Fukuda et al., 2003). The two types of thermal striping mixing tee experiments were led by Hitachi Ltd. and Toshiba corporations. The experiments led by Hitachi were performed for a co-current type mixing tee configuration where the hot coolant flow enters from the branch pipe and the cold coolant flow enters from one end of the main pipe. Experiments led by Toshiba simulated a collision type mixing tee. For this configuration, hot and cold coolant flows enter from both sides of the main pipe, and the mixing flow exits the tee junction through the branch pipe.

3.1. Co-current type mixing tee experiment

Fig. 1 is a schematic of the co-current type thermal striping experiments which were visualization tests in a mixing tee. The tee junction was constructed of acrylic pipes. The inner diameters of both the main and branch pipes were 10 cm. Hot water entering from the branch pipe was injected with methylene blue to allow visual observation of the coolant mixing. Cold water entered from one end of the main pipe. This type of thermal striping experiments in tee junction is dubbed *co-current* type. Thermocouples were installed at various near-wall locations of the pipes. The tips of the thermocouples were 3 mm into the coolant from the inner pipe wall. In addition to the axial locations parallel to the mixing flow direction (measured in L/D), thermocouples were installed at azimuthal locations of 0° (top), 45°, 90° (side), and 180° (bottom). The temperatures at each thermocouple location were recorded at a frequency of 25 Hz. Velocities and temperatures at the main and branch pipes were confirmed to be at steady-state before each experiment was performed (Kawamura et al., 2003).

3.2. Collision type mixing tee experiment

Fig. 2 is a schematic of the collision type thermal striping experiments. Similar to Hitachi's experiments, the Toshiba experiments were visualization tests of thermal striping with water coolant in a mixing tee. The tee junction was constructed of 10 cm ID acrylic pipes. The coolant flow entered from both ends of the main pipe and exited through the branch pipe. This type of thermal

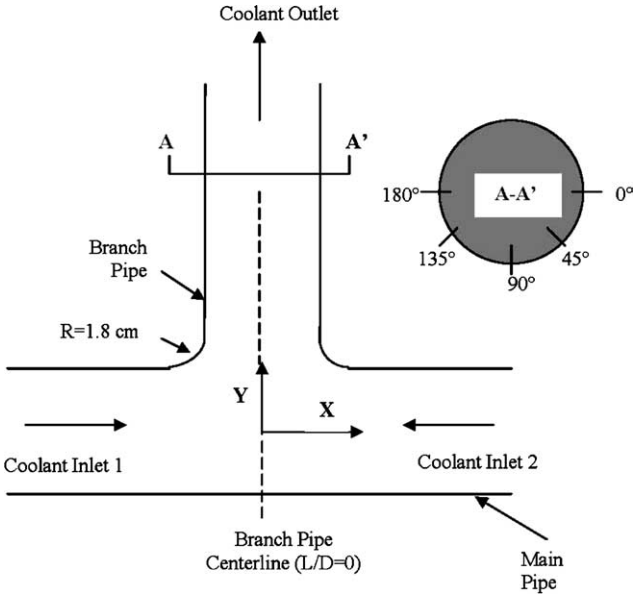

Fig. 2. Schematic of collision type thermal striping experiment in a mixing tee.

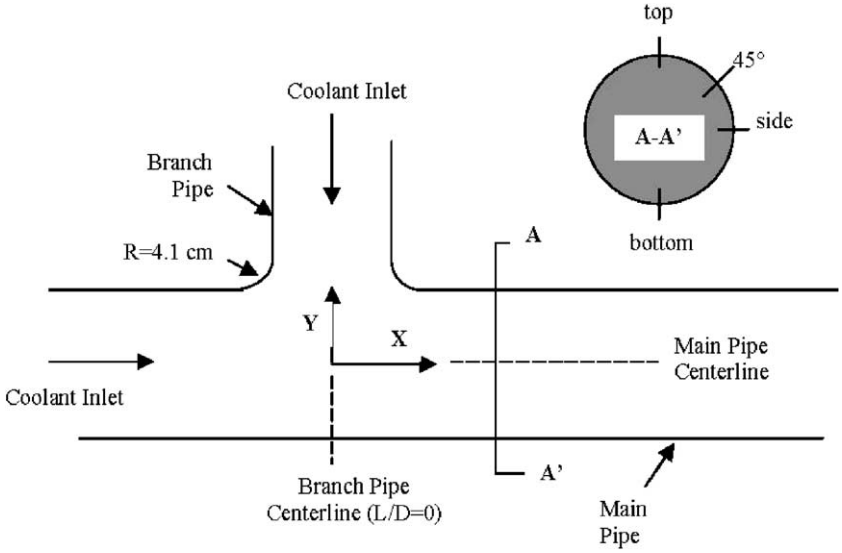

Fig. 1. Schematic of co-current type thermal striping experiment in a mixing tee.

striping experiments in tee junction is dubbed *collision* type. Thermocouples were installed at 0°, 45°, 90°, 135°, and 180° around the branch pipe at various axial locations along the pipe measured in L/D. The tips of the thermocouples were also located 3 mm into the coolant from the inner pipe wall. Sampling frequency of the thermocouples is not specified in the reference (Kimura et al., 2002).

The measured coolant temperatures at each thermocouple location were reported as normalized mean temperatures and normalized fluctuating temperatures. These normalized parameters were used elsewhere, as in Kimura et al. (2002), and are adopted here. The normalization parameter is the maximum ΔT, the temperature difference between the inlets of the hot and cold coolant flow, as shown in the following equation:

$$T^* = \frac{(T - T_{\text{cold}})}{(T_{\text{hot}} - T_{\text{cold}})} \tag{7}$$

where T is the instantaneous coolant temperature at a given location, T_{cold} is the temperature of the cold coolant flow, and T_{hot} is the temperature of the hot coolant flow. The time-averaged normalized mean temperature at a given location is:

$$\overline{T^*} = \frac{1}{N}\sum_{i=1}^{N} T^* \tag{8}$$

where N is the total number of sampling points.

The normalized fluctuating temperature, or the time-averaged temperature fluctuation intensity, is defined as the root-mean square of the instantaneous coolant temperature at a given location:

$$T^*_{\text{RMS}} = \sqrt{\frac{1}{N}\sum_{i=1}^{N}\left(T^*_i - \overline{T^*}\right)^2} \tag{9}$$

The parameters of the thermal striping experiments are shown in Table 1. The range of Reynolds numbers for these experiments in the mixing zone is about 300,000–600,000.

4. Benchmark study of mockup experiments

The three-dimensional tee junction models that represent the co-current and collision type experiments, as shown in Figs. 1 and 2, were constructed with GAMBIT, a pre-processor of the FLUENT code. Computational grids were generated with fine meshes in order to resolve the small-scale eddies in the near-wall area. An adiabatic wall boundary condition is applied in the FLUENT model of the benchmark experiments. This assumption is based on the fact that the pipe wall is acrylic that has very low thermal conductivity. Furthermore, the pipe wall is not modeled since the heat transfer through the pipe wall is negligible.

Procedures of the LES simulation are summarized as follows:

(1) Fully-developed boundary velocity profiles for the main and branch pipes were calculated using single pipe models. The Reynolds Stress turbulent model (RSM) was used for these simulations. The fully developed velocity profiles for the inlet main and branch pipes were written as boundary condition files to be used in the second step as the inlet velocity-boundary conditions.
(2) The tee junction geometry was constructed and the length of the main pipe downstream was initially set at $L/D > 15$. The meshes were coarser than the final meshes to allow rapid convergence. The purpose of this simulation is to determine the minimum length of the main pipe downstream that needs to be modeled. The criterion is that no reverse flow occurs at the outlet boundary. It was determined from the RSM calculation that the minimum required length is about 90 cm.
(3) A second tee junction mesh file was generated using a shorter inlet main pipe, outlet main pipe, and branch pipe in order to minimize the number of meshes. The meshes were finer than the previous case especially in the near-wall region. The first layer thickness was 0.1 mm with a growth ratio

Table 1
Experiment conditions of thermal striping mockup experiments

ID	Hitachi experiments (co-current type mixing tee)				
	Main pipe velocity (m/s)	Coolant temperature—main pipe (°C)	Branch pipe velocity (m/s)	Branch pipe temperature (°C)	Velocity ratio K ($=V_b/V_m$)
Case #H17	0.27	20.0	1.26	52.9	4.70
Case #H18	0.51	17.7	2.52	51.8	4.92
Case #H10	1.27	20.3	0.21	51.9	0.21
Case #H11	2.54	24.8	0.51	56.5	0.20
	Toshiba experiment (collision type mixing tee)				
	Inlet-1 velocity (m/s)	Inlet-1 coolant temperature (°C)	Inlet-2 velocity (m/s)	Inlet-2 coolant temperature (°C)	Velocity ratio K ($=V_1/V_2$)
Case #T1	2.5	60	0.5	20	5.0

of 1.2, and the maximum cell thickness in the main flow region was 3 mm. The total computation cells for this geometry were about 1,300,000 for both co-current and collision type experiments.

(4) The inlet-velocity profiles generated in the first step were attached to the main pipe and branch inlet boundaries. The RSM model was then used to obtain a steady-state solution.

(5) LES was initiated using the previously converged RSM solution as the initial condition. A constant time step size of 1 ms was used for thermal striping simulation. The temperature fluctuations became statistically stable after about one mean flow residence time (~1 s).

The spatial discretization scheme selected for solving the momentum and energy equations is the central-differencing scheme. The second-order upwind scheme was initially evaluated for this study. Although the second-order upwind scheme has the advantage of numerical stability, it was found that it may unduly damp out the momentum and energy fluctuations. The computation effort associated with the use of the central-differencing scheme is much higher because of the unstable nature of the numerical scheme. The result is a small time-step size (1 ms) in order to achieve convergence in every time step. The coolant thermal properties were given as polynomial functions of the coolant temperature.

4.1. Grid resolution in near wall region

Since the coolant temperature fluctuations in the near-wall region is of primary concern in thermal striping thermal fatigue, it is prudent to ensure that the computational meshes are fine enough to resolve the small-scale turbulent motions in this region. In the near-wall region y^+, a dimensionless parameter, has been used in defining boundary layer regions and turbulent channel flow velocity profile.

The wall unit, y^+, is defined as the distance from the wall normalized by the viscous length scale:

$$y^+ \equiv \frac{y}{\delta_v} \tag{10}$$

where y is the distance to wall and the viscous length scale δ_v is denoted as

$$\delta_v = v \cdot \sqrt{\frac{\rho}{\tau_w}} \tag{11}$$

The wall shear stress τ_w is calculated by

$$\tau_w = \frac{f}{4} \cdot \frac{1}{2} \rho \overline{V}^2 \tag{12}$$

where f is the friction coefficient, $\overline{V}$ is the mean flow velocity, and ρ is the coolant density.

The McAdams friction factor correlation was developed for a smooth tube (Todreas and Kazimi, 1990):

$$f = 0.184 Re^{-0.25} \tag{13}$$

This correlation is applicable for Reynolds number (Re) within the range between 30,000 and 1×10^6.

The viscous sublayer, which is dominated by the viscous stress, is defined as $y^+ < 5$. The buffer layer, which is the transition between viscosity dominated and the turbulence-dominated regions, is defined as $y^+ < 30$. Beyond $y^+ > 50$ through $y = 0.05D$, the viscous contribution to the wall shear stress is diminishing (Pope, 2000).

Depending on the velocity and temperature, the first grid thickness of 0.1 mm in our FLUENT model correspond to $1 < y^+ < 20$ for the five benchmark cases

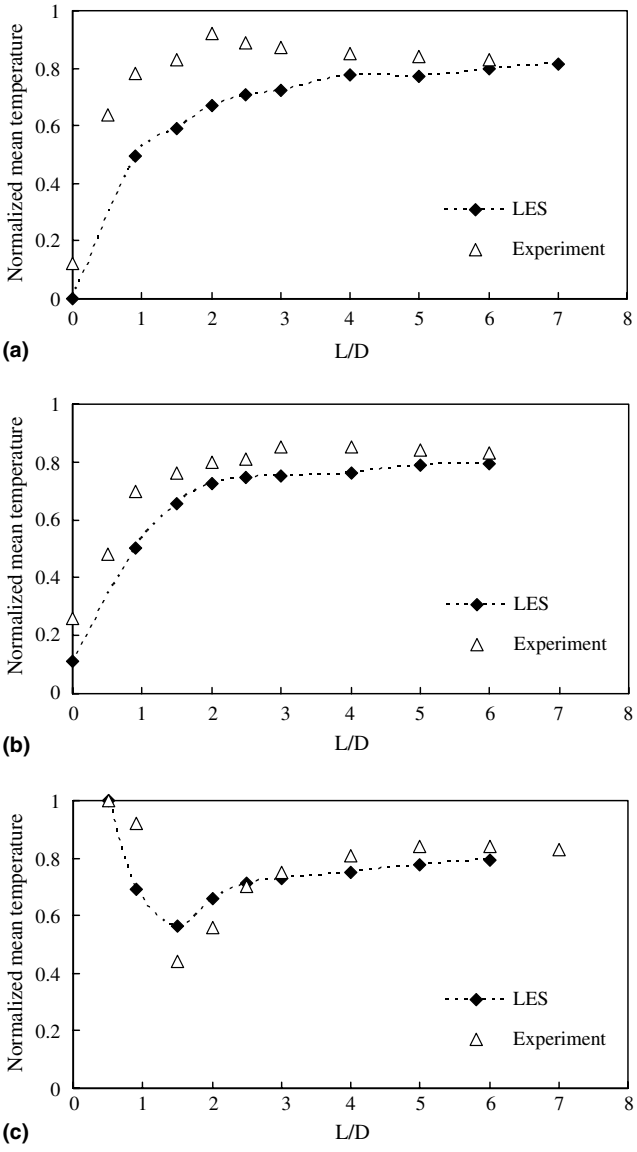

Fig. 3. Comparisons of measured and calculated normalized mean temperatures at: (a) bottom (180°), (b) side (90°), and (c) top (0°) for mockup experiment #H17.

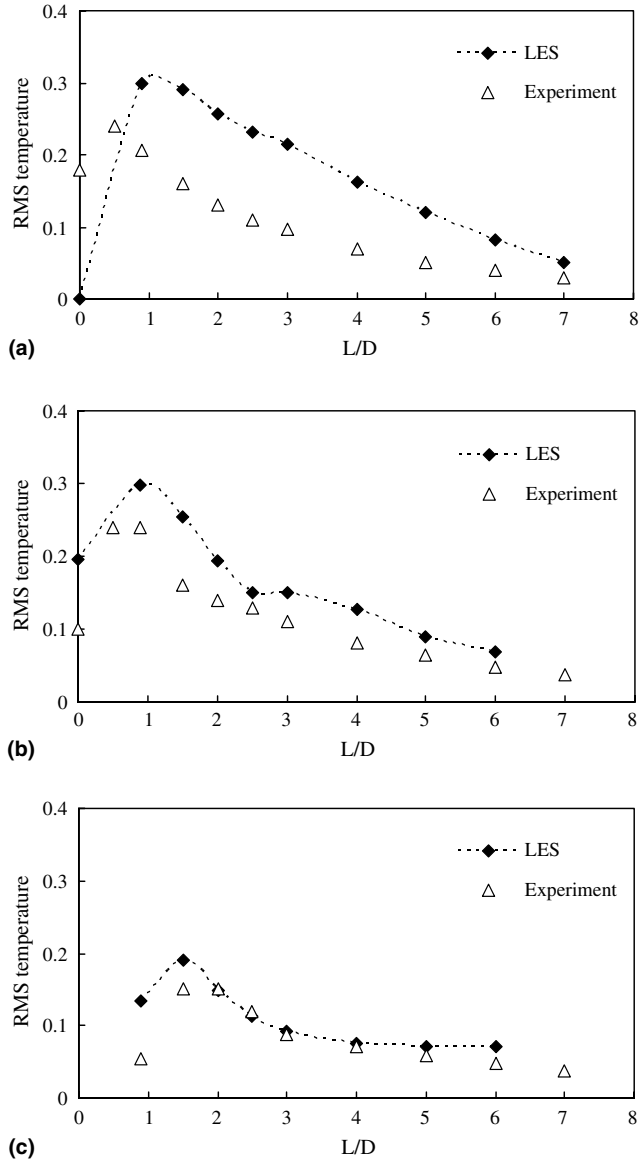

Fig. 4. Comparisons of measured and calculated normalized fluctuating temperatures at: (a) bottom (180°), (b) side (90°), and (c) top (0°) for mockup experiment #H17.

shown in Table 1. The subsequent grid spacing is set up using a growth factor of 1.2. The near wall region is sufficiently resolved and hence the near-wall model is automatically applied by FLUENT in the LES simulations.

4.2. Co-current type mixing tee simulation

4.2.1. Classification of flow pattern

Fig. 1 depicts a co-current type mixing tee. Depending on the momentum/velocity ratio of the entering flows, the turbulent mixing patterns can be further divided into "wall jet", "deflecting jet", and "impinging jet". Based on experimental observation, the types of mixing flow can be categorized using the momentum ratio of the main and branch pipe inlet flow (Igarashi et al., 2003).

$$M_R = \frac{\rho_m V_m^2 \cdot (D_m \times D_b)}{\rho_b V_b^2 \cdot \pi \cdot (D_b/2)^2} \tag{14}$$

where M_R is the momentum ratio, ρ is coolant density, V is velocity, D is pipe inner diameter, and subscripts m and b denote the parameters for main and branch pipes, respectively. Threshold for each flow pattern is defined as:

Wall jet	$M_R > 1.35$
Deflecting jet	$0.35 < M_R < 1.35$
Impinging jet	$M_R < 0.35$

"Wall jet" is characterized by a higher main pipe flow momentum so the branch pipe jet does not reach the center axis of the main pipe. The coolant temperature fluctuations occur only on the top half of the main pipe downstream of the mixing tee. "Impinging jet" corresponds to the condition where the branch pipe momentum is much higher than that of the main pipe and as a result the maximum coolant temperature fluctuations occur on the bottom of the main pipe downstream of the mixing flow. "Deflecting jet" occurs when the two inlet flows have comparable momentum.

Table 2
Comparison of the maximum normalized fluctuating temperatures

	Measurement			Calculation		
	Bottom (180°)	Side (90°)	Top (0°)	Bottom (180°)	Side (90°)	Top (0°)
Case #H17	0.24 (0.5)	0.24 (0.9)	0.15 (2)	0.30 (0.9)	0.30 (0.9)	0.19 (1.5)
Case #H18	0.21 (0.5)	0.22 (0.5)	0.15 (1.5)	0.30 (0.9)	0.32 (0.9)	0.21 (1.5)
	Side (90°)	45°	Top (0°)	Side (90°)	45°	Top (0°)
Case #H10	0.12 (0.9)[a]	0.18 (0.2)	0.1 (3)	0.21 (1.5)	0.24 (3)	0.18 (4)
Case #H11	0.1 (2.5)[a]	0.17 (0.2)	0.09 (3)	0.14 (4)	0.20 (2)	0.15 (4)

	0°	45°	90°	135°	180°	0°	45°	90°	135°	180°
Case #T1	0.25 (0.8)	0.27 (0.8)	0.27 (0)	0.17 (1.0)	0.19 (1.5)	0.35 (0.8)	0.33 (0.8)	0.29 (0.8)	0.31 (0.8)	0.28 (1.0)

The numbers shown in the parentheses are the L/D locations where the maximum normalized fluctuating temperatures occur. The largest L/D is shown if the maximum value occurs at more than one L/D location.

[a] The measured normalized fluctuating temperatures are in the range of 0.12–0.08 between $L/D = 0.9$ and $L/D = 7$.

The momentum ratio M_R is calculated to be 0.06, 0.05, 47.1, 32.0 for the four Hitachi experiments #H17, #18, #H10, #H11, respectively. As defined above, cases #H17 and #H18 correspond to "impinging jet" so the maximum temperature fluctuating is expected to occur in the lower half of the main pipe. Cases #H10 and #H11 are wall jets for which smaller temperature oscillations are expected because of relatively poor mixing pattern.

4.2.2. Simulation of impinging jet

Figs. 3 and 4 show comparisons of the measured and calculated normalized mean and fluctuating temperatures for experiment H#17. These normalized parameters were calculated using Eqs. (8) and (9). The results are shown for axial locations represented in L/D and circumferential locations of bottom (180°), side (90°), and top (0°). These locations correspond to those where thermocouples were installed in the experiment as shown in Fig. 1. The comparisons show good agreements of normalized mean temperatures with experimental data. In particular, a low temperature zone at the top of the junction is successfully captured by modeling as shown in Fig. 3(c). Coolant temperatures at the top, side, and bottom locations of the downstream flow approach that of a uniform mixing at $L/D \approx 3$. The cal-

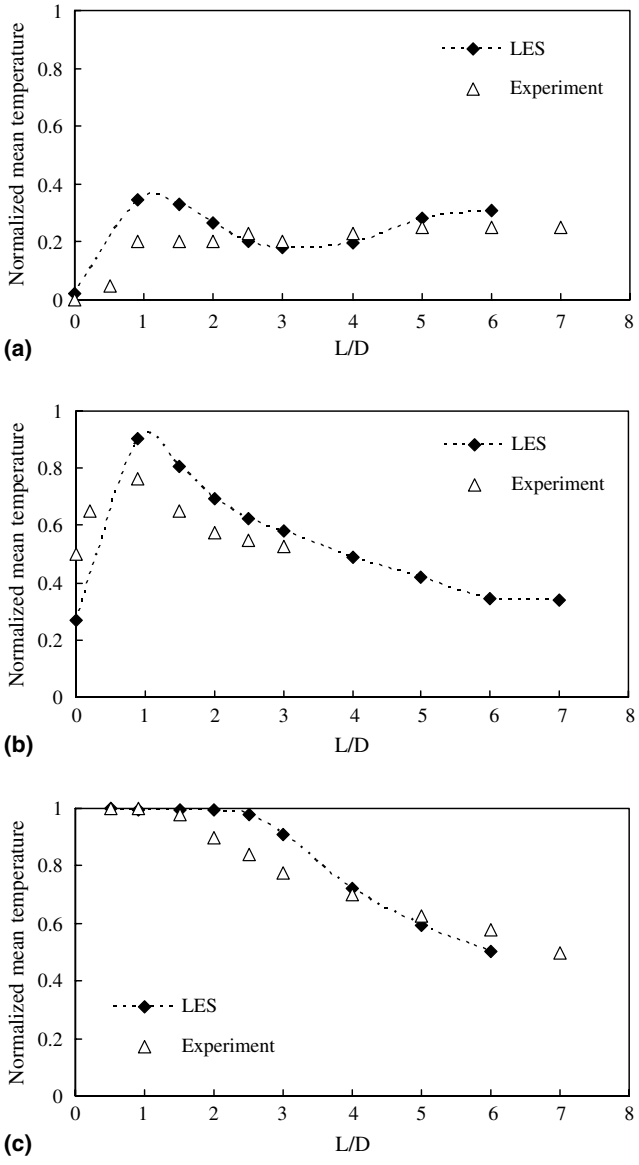

Fig. 5. Comparisons of measured and calculated normalized mean temperatures at: (a) side (90°), (b) 45°, and (c) top (0°) for mockup experiment #H10.

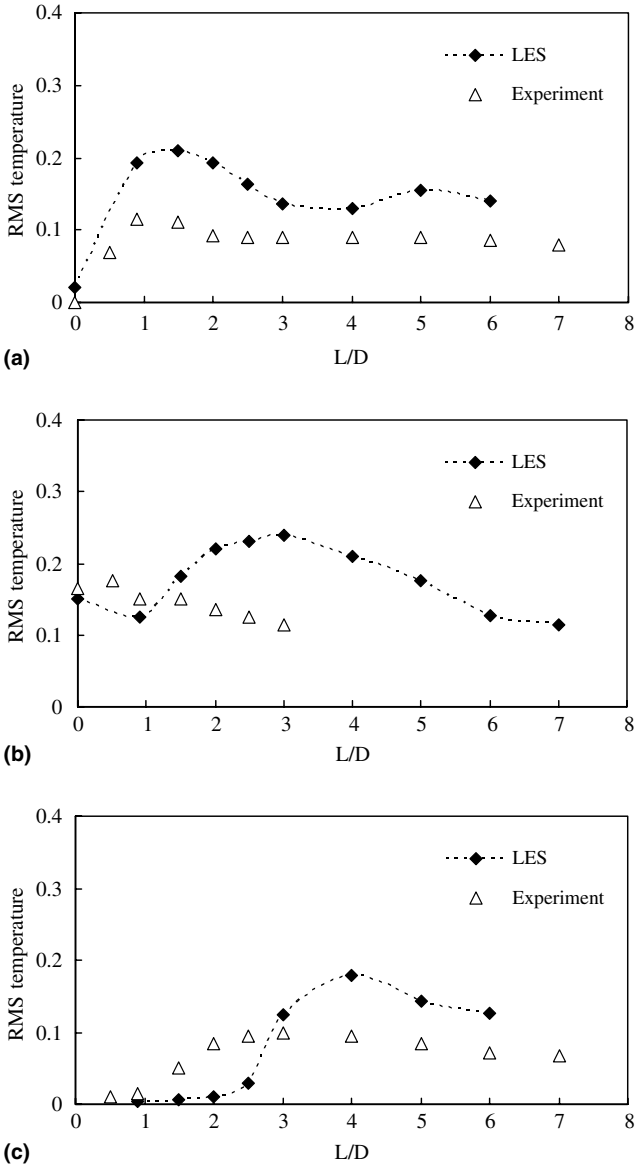

Fig. 6. Comparisons of measured and calculated normalized fluctuating temperatures at: (a) side (90°), (b) 45°, and (c) top (0°) for mockup experiment #H10.

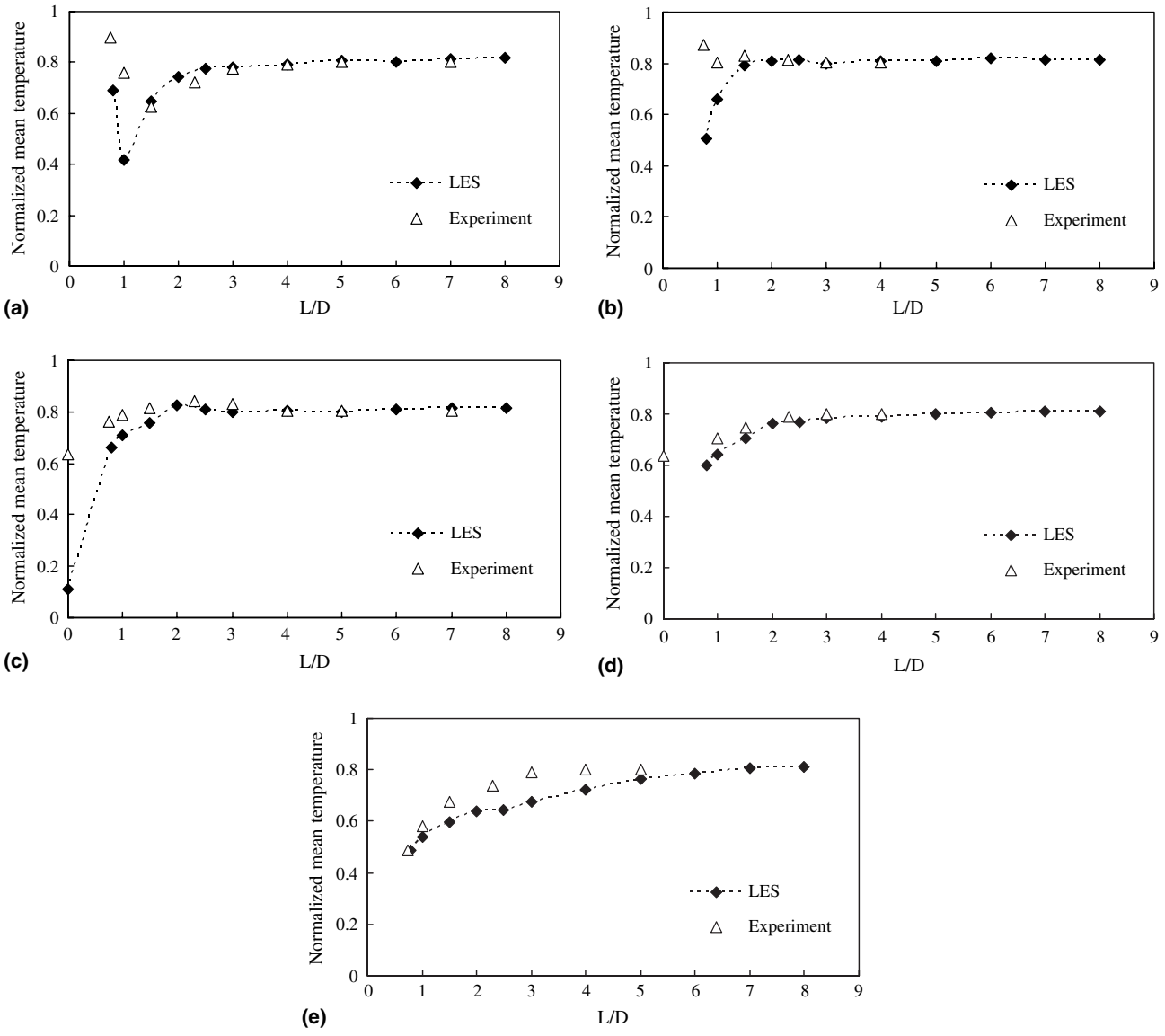

Fig. 7. Comparisons of measured and calculated normalized mean temperatures at: (a) 180°, (b) 135°, (c) 90°, (d) 45°, and (e) 0° for mockup experiment #T1.

culated peak fluctuating temperature locations are within about 0.5D to those obtained in experiments, and are generally higher than the experiments.

The experimental results obtained from Hitachi show a correlation of normalized mean and fluctuating temperatures with respect to the flow velocity ratios, i.e., the normalized mean and fluctuating temperatures plotted along the main pipe have similar trends as those of the same flow velocity ratio. Therefore, experiment H#18 is also modeled with the same procedures applied for case H#17. The comparisons of the experimental data and calculated results are similar to those of case H#17, which is the same as the experimental observation. Table 2 summarizes the magnitudes and locations of the maximum fluctuating temperatures. Calculated results for both cases are in good agreement with measurements. The peak maximum fluctuating temperatures occur at $L/D \approx 1$ and the bottom half of the main pipe at circumferential location of 180° and 90°.

4.2.3. Simulation of wall jet

Figs. 5 and 6 are comparisons of the measured and calculated mean and fluctuating temperatures for experiment H#10. The results are shown for circumferential locations of side (90°), 45°, and top (0°). Note the dominant temperature fluctuations were expected to occur on the top half of the main pipe because the main pipe inlet flow momentum is much higher than that of the branch pipe. Comparisons of normalized mean temperatures are in good agreements with experimental data. In contrast to the case of an impinging jet, the measured coolant temperature fluctuations are maintained

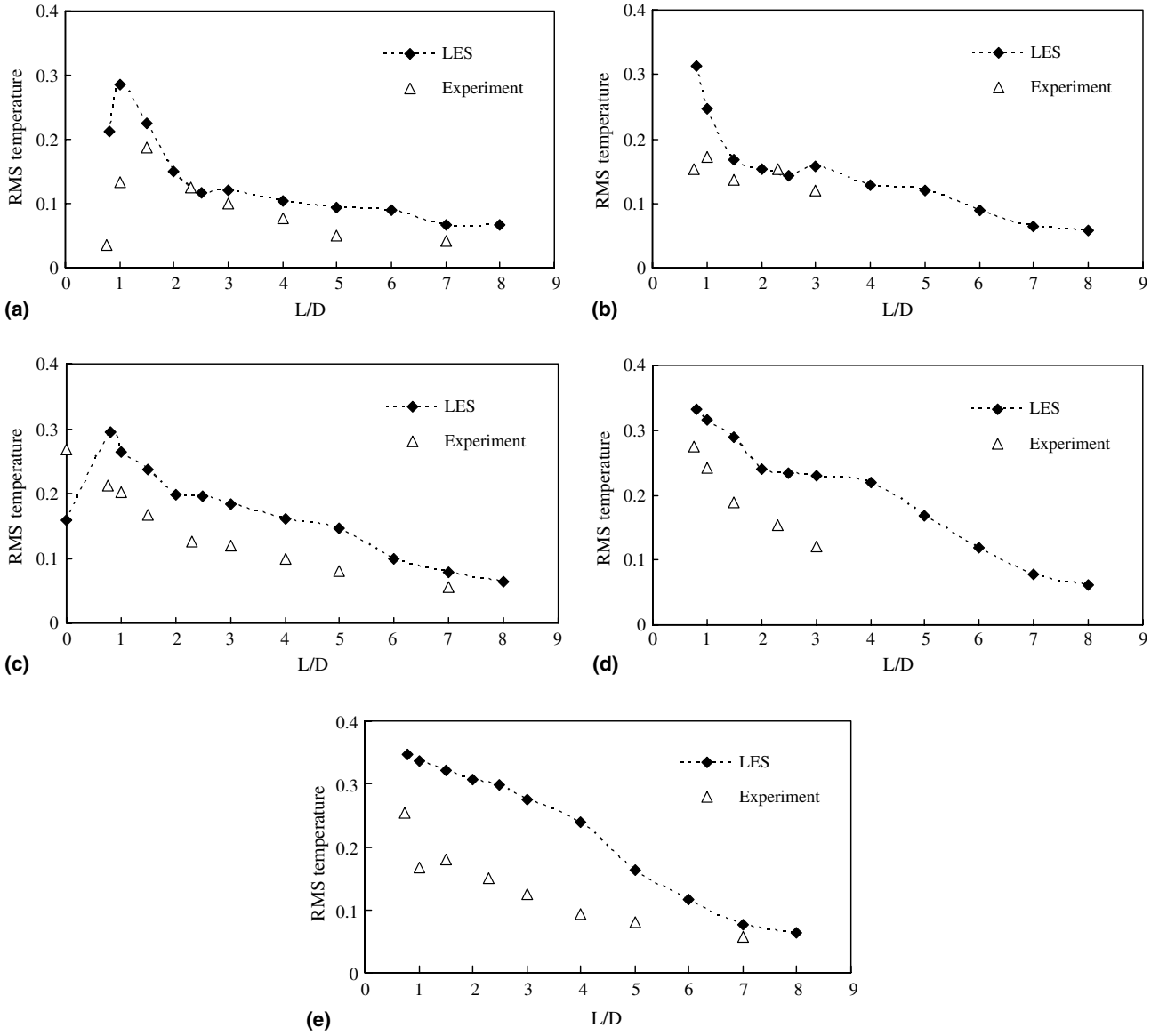

Fig. 8. Comparisons of measured and calculated normalized fluctuating temperatures at: (a) 180°, (b) 135°, (c) 90°, (d) 45°, and (e) 0° for mockup experiment #T1.

at almost a constant magnitude downstream of the tee junction. The LES simulation does capture the characteristics of a wall jet in predicting a lower-magnitude, sustained temperature fluctuations at all 3 radial locations downstream of the mixing tee.

Experiment #H11, which has the same velocity ratio as #H10, is modeled to investigate the velocity ratio effect. The comparisons of the experimental data and calculated results are similar to those of case H#10, which confirms the experimental observation. Comparisons of the magnitudes and locations of the maximum fluctuating temperatures are summarized in Table 2. The characteristics of nearly constant coolant temperature fluctuations at the 3 azimuthal locations are also observed as in the case H#10.

4.3. Collision type mixing tee simulation

The experiment parameters of the collision type mixing tee experiment #T1 is shown in Table 1. Wall boundary condition, coolant physical properties, numerical schemes, simulation procedures used in the Hitachi experiment simulations are adopted for the Toshiba experiment model. One notable difference in the geometry is that the Toshiba mixing tee experiment has a curvature of 1.8 cm at the junction compared to 4.1 cm of the Hitachi experiment. Also the main pipe and branch pipe lengths are set at 60 cm and 90 cm, respectively.

Fig. 7(a)–(e) are comparisons of the calculated and measured normalized coolant temperatures at five

circumferential locations of 180°, 135°, 90°, 45°, and 0° along the branch pipe. The thermal couples at 180° are closes to inlet-1 and those at 0° are closest to inlet-2 as depicted in Fig. 2. The calculated normalized mean temperatures are in good agreements with measurements for all five azimuthal locations and along the main pipe. One discrepancy noted is that LES had predicted a somewhat lower coolant temperature at $0.5 < L/D < 1$ and radial location of 135°. Fig. 8(a)–(e) are comparisons of the calculated and measured normalized fluctuating temperatures. The calculated normalized fluctuating temperatures are also in good agreements with measurements, with the calculated results being mostly higher than measurements. This is similar to what was observed in the Hitachi experiment benchmark study described in Sections 4.2.2 and 4.2.3.

Comparison of the peak normalized fluctuating temperatures and their corresponding locations for experiment #T1 are summarized in Table 2. The predicted locations of the maximum temperature fluctuations at the five azimuthal locations are within the range of 1D of measurements. While the experiment shows the maximum temperature fluctuations in radial locations from 0° to 90°, the calculation predicated the peak temperature fluctuations in the area from 0° to 90°.

No comparison can be made for the fluctuating frequency or power spectrum density, since the time histories of the measurements are not available. Furthermore, it is suggested that the thermocouples sampling frequency of 25 Hz in this experiment may not be adequate to resolve the high-frequency coolant temperature fluctuations. The thermal inertia and response time of the thermocouples may need to be taken in account for better comparisons between calculated and experimental results.

5. Conclusions

Three-dimensional, unsteady simulations of coolant temperature fluctuations in a mixing tee junction of the same diameter were performed using large eddy simulation (LES). Five sets of mockup experiments representing two types of mixing tee are used for this benchmark study. The calculated normalized mean temperatures and fluctuating temperatures are generally in good agreements with measurements. In particular, the locations of the maximum temperature fluctuations are predicated within the range of 1D of measurements.

The calculated maximum normalized fluctuating temperatures are somewhat higher than measurements. It is noted that the predicted coolant fluctuating temperatures and measurements are off in some cases. The possible causes for the discrepancy are: (a) the predicated coolant fluctuating temperatures are higher than measurement, and (b) the high-frequency temperature fluctuation components are not sufficiently resolved by the temperature measurements.

Our benchmark study demonstrated that LES is a promising tool to accurately analyze the coolant temperature fluctuations associate with high-Reynolds number turbulent mixing flows in a tee junction. It is shown that a multi-purpose commercial CFD software, such as FLUENT, can be applied in a complex thermal mixing problem if computational meshes, boundary conditions, numerical discretization scheme, and the SGS model are properly specified as described in this paper.

Acknowledgements

The authors would like to acknowledge Hitachi Ltd. for sharing their experimental data for the benchmark studies. Financial assistance for this project was provided by the Tokyo Electric Power Company (TEPCO).

References

Claude, F., 2003. Thermal fatigue in mixing tees: a step by step simplified procedure. In: 11th International Conference on Nuclear Engineering, ICONE-11, Tokyo, Japan, April 20–23.

Fukuda, T. et al., 2003. Current effort to establish A JSME code for the evaluation of high-cycle thermal fatigue. In: 11th International Conference on Nuclear Engineering, ICONE-11, Tokyo, Japan, April 20–23.

Hu, L.-W., Lee, J., Saha, P., Kazimi, M., 2003. Thermal striping in LWR piping systems, MIT-NSP-RP-017, MIT Center for Advanced Nuclear Energy Systems.

Igarashi, M., Kimura, N., Tanaka, M., Kamide, H., 2003. LES Analysis of fluid temperature fluctuations in a mixing tee pipe with the same diameters. In: Proc. 11th Int. Conf. On Nuclear Engineering ICONE-11, Tokyo, Japan, April 20–23.

Kawamura, T. et al., 2003. Study on high-cycle fatigue evaluation for thermal striping in mixing tees with hot and cold water. In: 11th Int. Conf. Nuclear Engineering, ICONE-11, Tokyo, Japan, April 20–23.

Kim, J.H., Roidt, R.M., Deardorff, A.F., 1993. Thermal stratification and reactor piping integrity. Nuclear Engineering and Design 139, 83–95.

Kimura, K. et al., 2002. Thermal striping in mixing tees with hot and cold water (Type A; Characteristics of flow visualization and temperature fluctuations in collision type mixing tees with same pipe diameter), NTHAS3: Third Korea-Japan Symposium on Nuclear Thermal Hydraulics and Safety (NTHAS3), Korea, October 13–16.

Lilly, D.K., 1966. On the application of the eddy viscosity concept in the inertial subrange of turbulence, NCAR Manuscript 123.

Muramatsu, T., Ninikata, H., 1996. Development of thermohydraaulics computer programs for thermal striping phenomena. Nuclear Technology 113, 54–72.

Ohtsuka, M. et al., 2003. LES Analysis of Fluid Temperature Fluctuations in a Mixing Tee Pipe with the Same Diameters, Proc. 11th Int. Conf. On Nuclear Engineering ICONE-11, Tokyo, Japan, April 20–23.

Pope, S., 2000. Turbulence Flow. Cambridge University Press.

Roubin, P.H.L., 1998. Temperature fluctuations in a pipe downstream a T junction. In: 9th meeting of the IAHR Working Group on Advanced Nuclear Reactor Thermal Hydraulics, Grenoble, France, April.

Smagorinsky, J., 1963. General circulation experiments with the primitive equations. I. The basic experiment. Monthly Weather Review 91, 99–164.

Todreas, N.E., Kazimi, M., 1990. Nuclear Systems I—Thermal Hydraulic Fundamentals. Hemisphere Publishing Corp.

Wakamatsu, M., Nei, H., Hashiguchi, K., 1995. Attenuation of temperature fluctuations in thermal striping. Journal of Nuclear Science and Technology 32 (8), 752–762.

Yakhot, A., Orszag, S.A., Yakhot, V., Israeli, M., 1989. Renormalization group formulation of large-eddy simulation. Journal of Scientific Computing 4, 139–158.